

## Article

# Enhanced Groundwater Protection and Management Using Gravity and Geoelectrical Data (Valls Basin, Spain)

Alex Sendrós <sup>1,2</sup>, Mahjoub Himi <sup>1</sup> , Lluís Rivero <sup>1,2,\*</sup> , Raúl Lovera <sup>1,2</sup>, Aritz Urruela <sup>1</sup> , Josefina C. Tapias <sup>2,3</sup>  and Albert Casas <sup>1,2</sup> 

<sup>1</sup> Department of Mineralogy, Petrology and Applied Geology, Universitat de Barcelona, 08028 Barcelona, Spain; alex.sendros@ub.edu (A.S.); himi@ub.edu (M.H.); rlovera@ub.edu (R.L.); aritz.urreuela@ub.edu (A.U.); albert.casas@ub.edu (A.C.)

<sup>2</sup> Water Research Institute, Universitat de Barcelona, 08001 Barcelona, Spain; jtapias@ub.edu

<sup>3</sup> Department of Biology, Health and Environment, Universitat de Barcelona, 08028 Barcelona, Spain

\* Correspondence: lrivero@ub.edu

**Abstract:** The basis for the protection and prevention of groundwater pollution lies in the accurate assessment of vulnerability in terms of the exposure of groundwater bodies to contaminants before they are potentially discharged into the environment. The vulnerability assessment consists of calculating the ease with which pollutants can reach the aquifer from the surface through the vadose zone, which effectively reduces the pollutant load when the transit time is long. Index methods are mostly used, as they are based on input data that are readily available, easy to implement and interpret, and which are simple and practical. However, there are also limitations, as some methods are somewhat subjective and provide only a qualitative approximation. This case study aims to develop a methodology that can quantitatively estimate the hydrogeological parameters of the aquifer formations of the Valls basin using geophysical methods and the Dar Zarrouk parameters. The specific treatment carried out on data from gravity stations and vertical electric soundings, supported by the available well data, allows for the delineation of the most favourable areas for the exploitation of groundwater resources (higher hydraulic transmissivity) and the areas most susceptible to pollution (with a shorter transit time) on a regional scale. Geophysical methods have proved useful, sustainably providing valuable information without the need to drill new boreholes that could act as preferential pathways for pollutants into the aquifer.

**Keywords:** vulnerability mapping; groundwater protection; hydrogeophysics; electrical resistivity methods; gravity survey; aquifer transmissivity



**Citation:** Sendrós, A.; Himi, M.; Rivero, L.; Lovera, R.; Urruela, A.; Tapias, J.C.; Casas, A. Enhanced Groundwater Protection and Management Using Gravity and Geoelectrical Data (Valls Basin, Spain). *Water* **2023**, *15*, 4130. <https://doi.org/10.3390/w15234130>

Academic Editor: Chin H Wu

Received: 3 November 2023

Revised: 24 November 2023

Accepted: 27 November 2023

Published: 28 November 2023



**Copyright:** © 2023 by the authors. Licensee MDPI, Basel, Switzerland. This article is an open access article distributed under the terms and conditions of the Creative Commons Attribution (CC BY) license (<https://creativecommons.org/licenses/by/4.0/>).

## 1. Introduction

The European Orders relating to the protection of water from pollution, the Directive 2000/60/CE of the European Parliament and the European Union Council [1], and, more specifically, Directive 2006/118/CE [2], relate to the protection of groundwater from pollution and degradation, demonstrating that subsurface water protection has emerged as one of the most significant environmental policies in Europe. The basis for protection and prevention lies in an accurate assessment of the vulnerability of aquifers in terms of the exposure of groundwater bodies to pollutants potentially discharged into the environment, particularly on the ground's surface. A vulnerability assessment consists of calculating the ease with which pollutants reach the aquifer from the surface, crossing through the unsaturated subsurface (or vadose zone) since the time required for the pollutant to reach the aquifer has a direct effect on the amount of pollutant that can eventually be incorporated into the groundwater [3,4]. Several mechanisms (aerobic biodegradation, volatilisation, adsorption in the solid matrix) take place in the unsaturated zone, which effectively reduces the pollutant load when the transit time is long [5–7].

According to Gogu & Dassargues [8], the assessment of vulnerability is limited to a given site or area and depends mainly on the recharge, soil properties, and characteristics of the unsaturated zone alongside the characteristics of the aquifer itself. It also depends secondarily on the topography, the relationship between the surface water and groundwater, and, in the case of multilayer aquifers, the nature of the underlying aquifer units.

The concept of groundwater vulnerability is based on the assumption that the physical environment provides the natural protection of groundwater against human impacts, especially concerning the pollutants introduced from the ground's surface [9].

The degrees of vulnerability to contamination can be expressed in maps that allow a simple and intuitive representation of their spatial variability and are particularly useful in land-use planning processes [10]. Their primary goal is to make it easier to manage land use properly, based on regional underlying conditions, and prevent groundwater pollution, as cleaning up contaminated areas may be costly, time-consuming, and even impossible [11].

Index methods such as DRASTIC [12], GOD [3], SINTACS [13], and GALDIT [14] are the most commonly used vulnerability assessment methods as they are based on input data that are readily available, easy to implement, and interpret, as well as being simple and practical [15,16]. However, there are also limitations, as some methods are somewhat subjective in assigning numerical values to the descriptive entities and relative weights for different attributes and provide only a qualitative approximation [17].

This is especially concerning for aquifers in protected regions since there is typically a lack of direct information regarding subsurface conditions and, thus, a lack of other subsurface data and additional subsurface data are required to supplement the surface geological data, such as those obtained using indirect geophysical methods.

Soil surveys, drilling, and the examination of lithology logs from wells are conventional techniques for assessing groundwater vulnerability. The goal is to characterise the protective layers' thickness, hydraulic characteristics, and lateral extent. These studies, however, can be costly and labour-intensive too. Furthermore, precise parameter measurements over broad areas might be challenging due to the considerable spatial variability of concerning data [18].

Thankfully, the longitudinal electrical conductance parameter easily obtained from vertical electrical resistivity surveys (VES) may be used to assign a numerical index of protection as it could provide accurate information about the thickness, depth, and lateral continuity of clayey-dominated layers that act as natural barriers [19]. The results of these measurements can be used to estimate the clay content and vertical hydraulic conductivity of the non-saturated zone or to interpolate vulnerability indices quantified by rating systems such as the Aquifer Vulnerability Index between wells [20]. Compared to existing vulnerability indices that are only based on a visual inspection or interpolated from scarce borehole data, the use of geophysical data has the potential to be more accurate and dependable [21–24].

Moreover, using the transverse resistance parameter, which is also easily obtained from the inversion of VES curves, can be correlated with the aquifer hydraulic transmissivity parameter [25–28], allowing us to indirectly characterise the rate of the lateral flow of groundwater as a complement to pumping tests that form well [29].

This case study aims to develop a methodology that can estimate hydrogeological parameters in the aquifer formations of the Valls basin using geophysical methods, including the Dar Zarrouk parameters, to delineate the most favourable areas for the exploitation of subsurface water resources (higher hydraulic transmissivity) and the areas most susceptible to pollution (shorter transit time).

## 2. Studied Zone

The studied zone is situated in the Alt Camp district of the Spanish province of Tarragona, between the Gaià and Francolí rivers, and around 100 kilometres south of Barcelona

city (Figure 1). With a surface area of about  $320 \text{ km}^2$ , it is morphologically a wide plateau following a northeast–southwest axis and bordered by the Catalan System's Ranges.

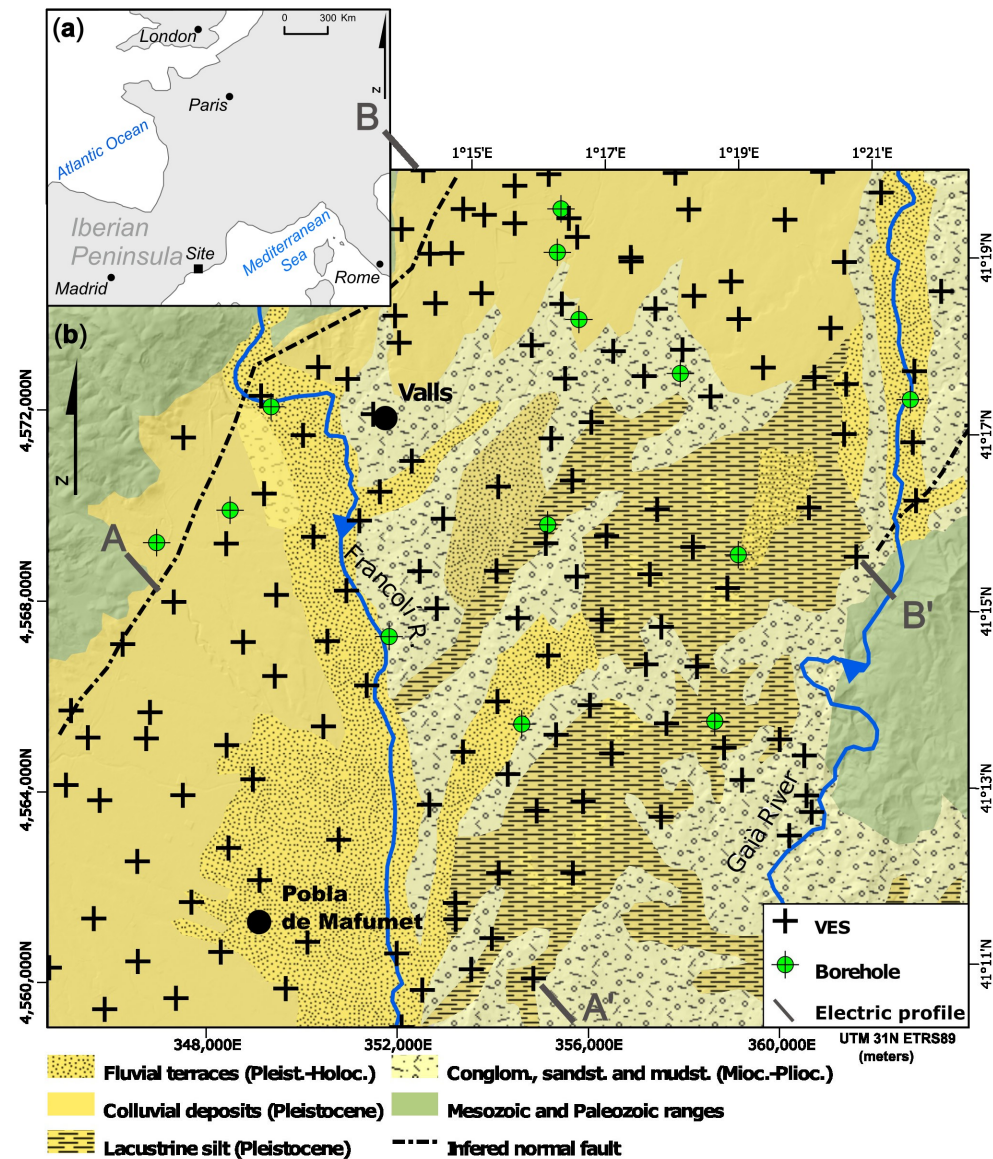


**Figure 1.** (a) Location sketch of the studied zone; (b) Geological setting, geophysical data (vertical electrical sounding—VES) and borehole distribution. Base map modified from [30].

Most of the basin is covered by an upper alluvial aquifer with considerable heterogeneity and anisotropy, especially in the flat parts and the sectors along the Francolí and Gaia rivers, where some fluvial terraces are discernible [31]. High transmissivity gravels in a range of particle sizes compose the alluvial deposits. Although the Plio-quaternary aquifer is unconfined in many places, hydrogeological barriers are generally produced by the presence of clayey sediments. As a result, it can be referred to as a multi-layered complex aquifer with significant lateral variations in transmissivities between its sides. Three layers of sand and gravel, interbedded with silt and clay layers of varying thickness, can be considered as the site aquifer system [32]. The groundwater from both aquifers contains significant concentrations of nitrogenous compounds due to the agricultural use of over 60% of the surface. In the past, from 1969 to 1989, the average nitrate content in water drawn from wells in the Francolí alluvial aquifer was approximately  $15 \text{ mg/L}$ . This amount has since risen to over  $50 \text{ mg/L}$ . The wells that were monitored by the Catalan Water

Agency in 2022 showed nitrate concentrations ranging from below 5 mg/L to 175.6 mg/L, with a well close to the town of la Pobla de Mafumet having the highest concentrations [33].

Currently, the multilayer aquifer system has a strategic awareness of water supply, and the interest of its study is complemented by the fact that it is an area declared partially vulnerable to diffuse nitrate pollution [34], and there is no representative subsoil data of all of the studied site (only 13 boreholes mainly clustered on the north zone).

### 3. Materials and Methods

#### 3.1. Gravity Survey

Gravity prospecting is based on the measurement of variations in gravity acceleration due to the distribution of rocks with different densities in the subsurface. It is a fast and relatively inexpensive natural field method that is usually applied in the preliminary stages of many subsurface surveys [35].

This methodology consists of measuring gravity values in a grid of points covering the area to be explored and employing an instrument called a gravimeter (Figure 2), which can measure gravity differences between two points with high sensitivity (about 0.01 mGal). As gravimeters are relative instruments, the measurements are made with the classic closed-loop system with the start and end of each itinerary on a gravity base with an absolute gravity value linked to a reference system; in our case, this was the International Gravity Standardization Net (IGSN'71). In addition, these measurements at the beginning and end of each route are used to carry out the instrumental drift and to test the general response of the gravimeter.

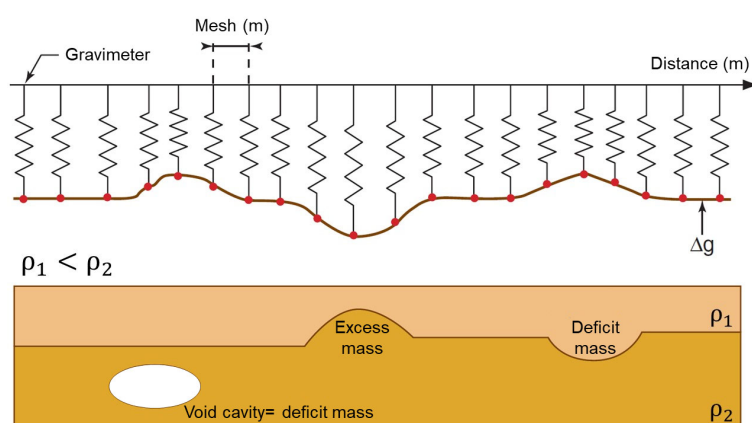


**Figure 2.** Gravimetry principle: the variation in the density of the subsoil generates a variation in the gravitational field ( $\vec{g}$ ). Modified form [36].

To obtain the neutral gravity values at each point (i.e., without the additional attraction effect of the sun and the moon), the gravity tidal effect is calculated numerically. The gravity tide values oscillate periodically between +0.15 and −0.15 mGal, with two daily maxima and two daily minima. After subtracting the lunisolar effect, the difference in readings at the base at the beginning and end of each itinerary is compensated proportionally to the time spent at each station as instrumental drift.

As the gravity at a particular point is a function of different factors, instead of the absolute value of gravity, the variable of interest is the so-called Bouguer Anomaly (BA), which can be defined as the difference between the measured gravity value and the normal or expected gravity value. This normal or expected value can be calculated theoretically from a mathematical model, which involves the calculation of normal gravity on the reference ellipsoid as a function of geographical latitude and the transport of this value from the ellipsoid to the conditions of the station on the earth's surface, taking into account the influence of the height of the station, the average density of the rocks and the relief around the point of measurement. Once the value of gravity on the ellipsoid has been calculated as a function of geographical latitude, it must be transferred to the ground's

surface to compare it with the observed gravity value and obtain the parameter of interest, BA [37].

### 3.2. Geoelectrical Survey

Direct current electrical methods, and, in particular, the technique known as vertical electrical sounding (VES), have been widely used due to the high electrical conductivity and contrast of geological and hydrogeological units [38–41]. This technique consists of injecting an electric current into the ground through two electrodes (current electrodes also noted as A and B) and measuring the voltage difference through two other electrodes (potential electrodes). There are different geometrical configurations for placing the electrodes in the ground, which have given rise to different measuring arrays. The best known are the Schlumberger, Wenner, and Dipole–dipole arrays [35]. By taking these measurements at the surface, electrical surveys aim to determine the subsurface electrical resistivity distribution. When unconsolidated, the porosity and clay content both affect electrical resistivity (assuming all pores are saturated). Typically, sandy soil is more resistive than clayey soil. Nevertheless, there is an overlap in the values of many types of rocks and soil because a variety of parameters, including porosity, water saturation level, and dissolved salt concentration, influence a specific rock or soil sample's resistivity [42].

The Spanish Geological and Mining Survey (IGME) carried out an electrical prospecting campaign with the VES methodology in the Camp de Tarragona area (1981–1985). One hundred and forty-one of these VESs were selected from their database as they effectively covered the study area, forming an almost regular grid with two km spacing between them (Figure 1 and Supplementary Material S1). The VESs acquired after 80 s using a Schlumberger array (Figure 3) were able to reach great depths in the vertical (between 100 and 300 m) as well as great extensions on the horizontal surface of the terrain (between 500 and 1500 m electrodes A–B maximum distances) because of the topographic and less-urbanised conditions of the terrain at that time.

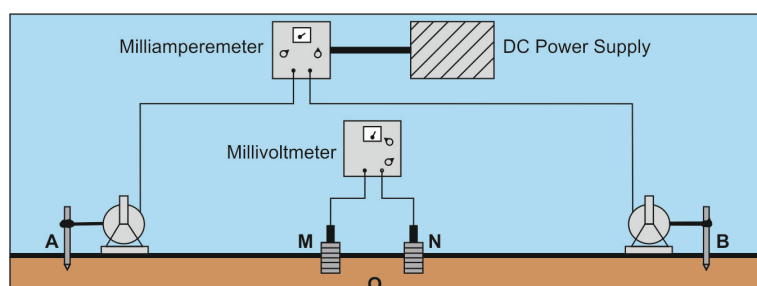


**Figure 3.** Sketch of VES acquisition using the Schlumberger array (modified from [42]). A–B are current electrodes, M–N are potential electrodes and O is the location of the measurement point.

The purpose of the quantitative interpretation of VES data was to obtain information on the thickness and electrical resistivity of the subsurface materials and the entire aquifer section. The data were inverted using REXIP Plus v2.53 software [43] to obtain the real resistivity distribution using ridge regression [44]. The initial conditions of each of the models with  $n$  layers,  $n$  values of electrical resistivity and  $n - 1$  thicknesses (since the last layer was assumed to be of infinite thickness) were established with the lithological columns available from the nearest mechanic boreholes to each of the VESs.

In the case of the VES closest to a borehole, the number of layers and the thickness were left as fixed and invariable variables during the inversion process, and each of the initially estimated resistivities and the thickness of layer  $n - 1$  as free parameters.

On the other hand, in the VES located away from a borehole, the inversion results of the VES close to a borehole are taken as the initial model. In this case, the number of layers was a fixed parameter, and the electrical resistivity, and the thickness of the layers were defined as variable parameters.

### 3.3. Dar Zarrouk Parameters

The fundamental electrical characteristics of stratified models known as Dar Zarrouk (DZ) parameters provide an in-depth understanding of the theory of the electrical behaviour of the subsurface. These are related to multiple combinations of resistivity and thickness for each geoelectrical layer in the model, which is an experimental VES curve that can be explained as produced by many physically equivalent models (principle of equivalence) [45]. The DZ parameters, longitudinal conductance ( $S$ ) and transverse resistance ( $T$ ) for a series of  $n$  horizontal, homogeneous, and isotropic layers with thickness  $h_i$  and resistivity  $\rho_i$ , are defined as follows:

$$T_i = h_i \cdot \rho_i$$

$$S_i = \frac{h_i}{\rho_i}$$

The approach used to calculate the  $T$  parameter of Dar Zarrouk was also the same as that used for the calculation of the hydraulic transmissivity parameter, i.e., it was computed from the piezometric level (W.T.) to the base of the aquifer (Figure 4). The base of the aquifer has been considered to be located at a maximum depth of 100 m. The 100 m limit was chosen because it is the depth of most calibration data used; in this case, the lithological log of boreholes, as well as the minimum investigation depth of VES soundings, were used [46].

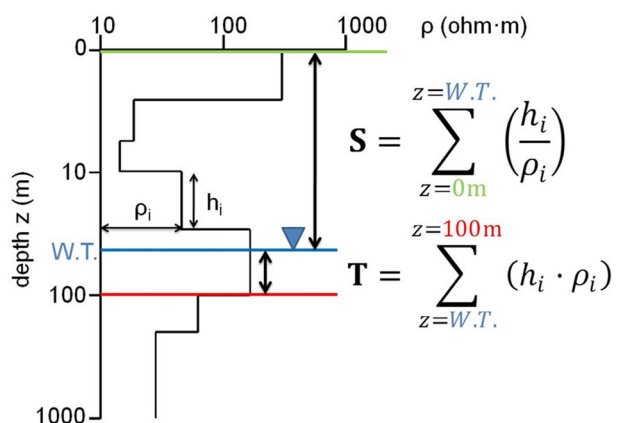


**Figure 4.** Diagram of the calculation carried out to obtain the  $S$  and  $T$  parameters of Dar Zarrouk.

The water table data were gathered from the groundwater control network of the Water Catalan Agency [47] and were interpolated using an ordinary kriging algorithm [48] implemented on Surfer v16 (Golden Software, Golden, CO, USA).

The evaluation of the Dar Zarrouk  $S$  parameter is computed from the ground surface to the piezometric level, considering that it has a maximum value when the thickness of the low resistive layers overlying the water-bearing formation is large, giving the aquifer high protection against contamination from the ground surface [49].

### 3.4. Vulnerability Assessment

The AVI (Aquifer Vulnerability Index) method was developed in Canada by the authors of [50] and attempts to assess vulnerability based on a physically based concept that consists of determining the hydraulic resistance ( $C$ ) or the time required for pollutants to cross the different layers between the ground surface and the aquifer (unsaturated zone). The hydraulic resistance is calculated based on the thickness of each of the  $i$  layers overlying

the aquifer ( $h$ ) and the estimation of the hydraulic conductivity of each of them ( $k$ ) using the following expression:

$$C_i = \frac{h_i}{k_i}$$

The AVI method is relatively simple to apply, allows for a semi-quantitative vulnerability assessment, and is less physically based. However, obtaining representative  $k$  values can be very costly. To overcome this limitation, the authors of [51] made a variation in the method and used the thickness ( $h$ ) and the resistivity ( $\rho$ ) of each of the layers of the unsaturated zone to obtain, in this case, the Dar Zarrouk parameter  $S$  representative of the vertical component of the electrical current through the unsaturated zone.

In addition, the authors obtained an empirical relationship of the value of  $S$  (in Siemens) with the time it would take for a pollutant to reach the aquifer (transit time).

The transit times through unsaturated layers are theoretically and linearly related to the longitudinal unit conductance ( $S$ ) of the layers, with an estimated standard deviation of 2.9 years. We used it to quantify the protective capacity of the underlying aquifers from percolating contaminants.

#### 4. Results and Discussion

##### 4.1. Gravity Survey

The geometry of a sedimentary basin is generally evident from the gravity anomalies generated by the mass deficit of the sediments with the basement rocks [52]. In the case of the Camp de Tarragona basin, the density contrast between the Neogene sediments and plutonic rocks, Palaeozoic schists, and Mesozoic limestones of the basement is significant and of the order of  $250 \text{ kg/m}^3$ . In order to determine the geometry of the basin, 1270 gravity stations available in the Camp de Tarragona area were reprocessed with Oasis Montaj v7.0.1 (Geosoft, Toronto, ON, Canada), and the regional trend was generated by the decrease in the thickness of the earth's crust, as shown in the map of gravity anomalies of the Catalonia region [53].

The residual anomaly map obtained was superimposed on the geological map of the area (Figure 5) with Surfer v16 (Golden Software, Golden, CO, USA). This shows the correspondence between the distribution of the negative gravity anomalies and the structural position of the basin. It also shows that the basin has two depocentres, one to the SW with negative gravity anomalies exceeding  $-18 \text{ mGal}$  and the other to the NE with a low gravity of  $-10 \text{ mGal}$ . Both depocentres are separated via a structural high that can act as a groundwater watershed.

##### 4.2. Geoelectrical Survey

Following the procedure presented in Section 3.2, the 141 apparent field VES curves and the 1D geoelectric layered models were obtained (Supplementary Materials S1 and S2), but, as a summary, only the simplified results of two opposite models of the field curves and VES models are presented in this section (Figure 6).

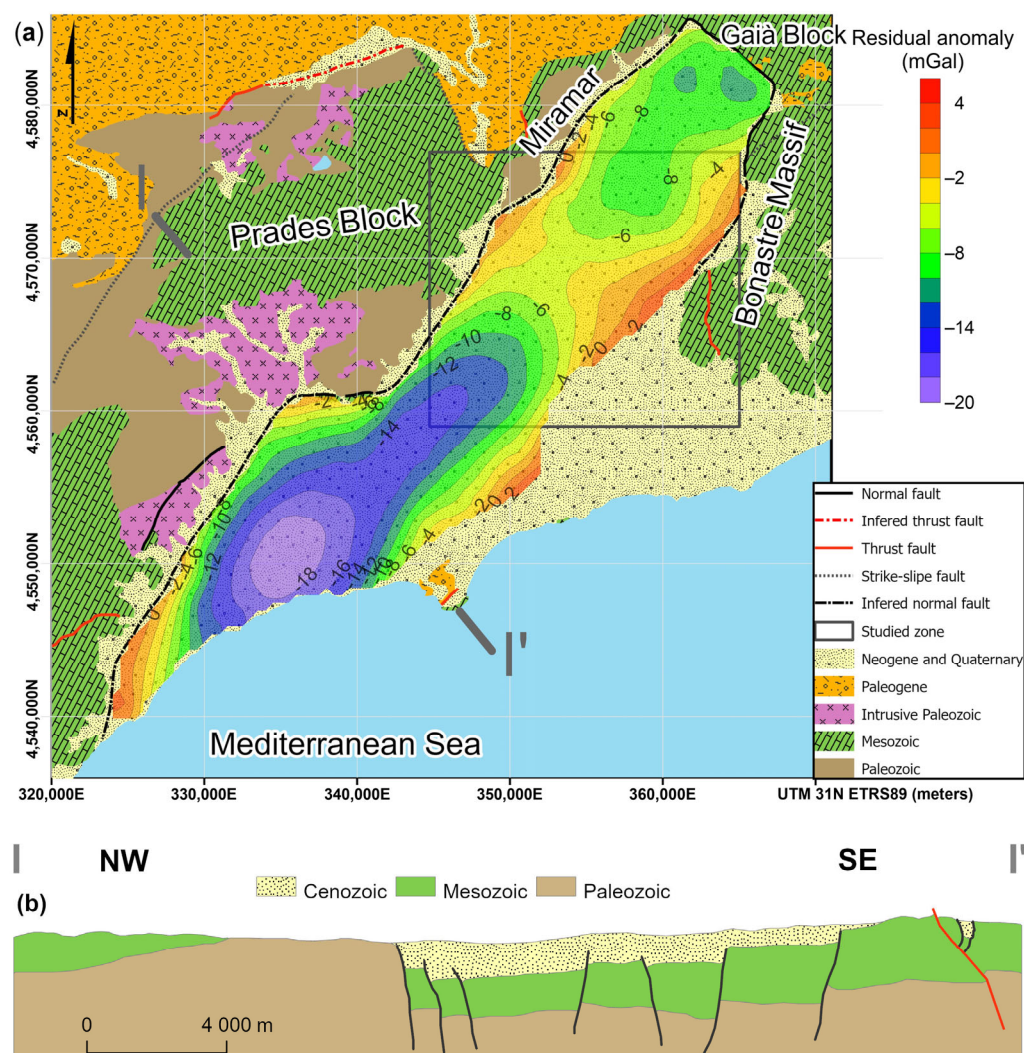


**Figure 5.** (a) Map of residual gravity anomalies of the Camp de Tarragona basin superimposed on the geological sketch of the area; (b) Geological profile I-I'. Modified from [54].

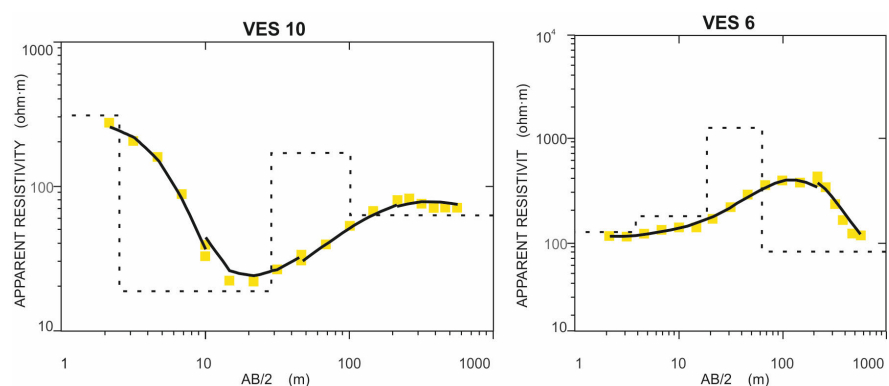


**Figure 6.** VES curves obtained in Valls site. Field data are presented with yellow squares: a VES model curve with black lines and a VES layered model as a black dashed line.

VES 10 is the typical H-curve showing a thick layer with low electrical resistivity values ( $10$  to  $20$   $\Omega\cdot m$ ), and VES 6 (K-type curve) shows intermediate electrical resistivity values (close to  $150$   $\Omega\cdot m$ ) above a layer with a high electrical resistivity response (over  $1000$   $\Omega\cdot m$ ).

There is a good correlation achieved between the field data and the electrical models. The estimation of the error between the field data and the electrical model obtained in the last iteration, with the inversion software, was between 1.1 and 11.7%, with an average error of less than 3.5% (Supplementary Material S1).

Moreover, with the data from 19 VES models, 2 electrical resistivity cross-sections perpendicular to the direction of the main geological structures were obtained. The IPI2Win software v3.0.1 [55] was used for their representation, and a general trend was identified in the study area of the increasing electrical resistivities of the subsurface from south to north (Figure 7).

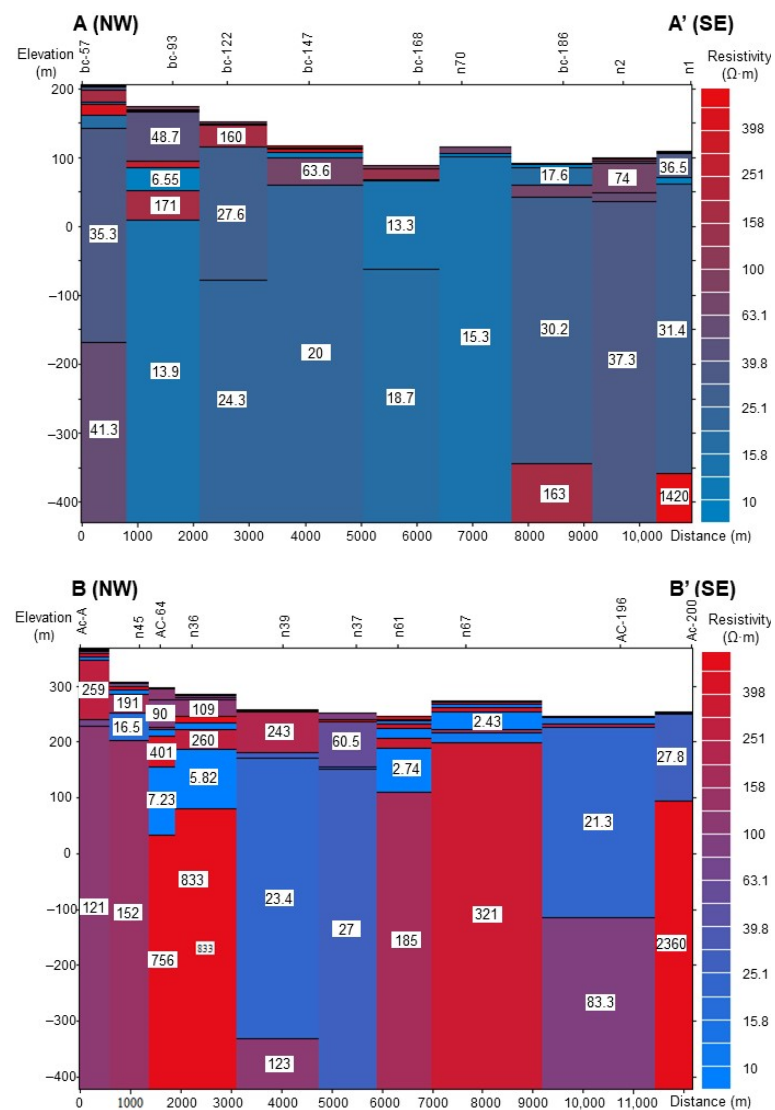


**Figure 7.** Electrical resistivity cross-sections and their geological interpretation obtained from 19 VES models at the studied zone. The reddish tones indicate high electrical resistivities and the blue tones indicate lower electrical resistivities.

The VES results are interpreted as clay layers interbedded with a variety of geologic sediments, including sand and gravel. The primary findings are the characterisation of the clay formations, as indicated by low-resistivity values ( $<50 \Omega \cdot m$ ) and sand layers linked to high-resistivity values ( $500 \Omega \cdot m$ ) that are located around the study site's boundaries.

#### 4.3. Hydraulic Transmissivity

The distribution of the Dar Zarrouk  $T$  parameter was plotted on a contour map. This map was produced with Surfer v16 (Golden Software, Golden, CO, USA) using the ordinary Kriging interpolation method. The interpolation was performed with a regular square grid of 30 m, limited to the areas with sufficient data and excluding those without values (NW and SE of the studied rectangle). The result was an isoline map in which two subgroups of values, those above 5000  $\Omega \cdot \text{m}^2$ , of transverse resistance values could be distinguished.

The values lower than 5000  $\Omega \cdot \text{m}^2$  were located and distributed with an approximate NE-SW orientation, in the central part of the studied area. Results higher than 5000  $\Omega \cdot \text{m}^2$  were identified in the northern and southern parts, also oriented NE-SW, and in the central-western sector with an N-S orientation.

In the IGME hydraulic transmissivity map, two subgroups could also be distinguished. In this case, one group had values above 200 (*fluvial terraces of the Gaià and Francolí rivers and the alluvial fan of Alcover*), and the other had values below 200  $\text{m}^2/\text{day}$  (*the rest of the formations*). The distribution of the two subsets of hydraulic transmissivities practically coincided with that of the two subsets of transverse resistances (Figure 8). This last fact shows the good correlation of both parameters at the working scale selected.

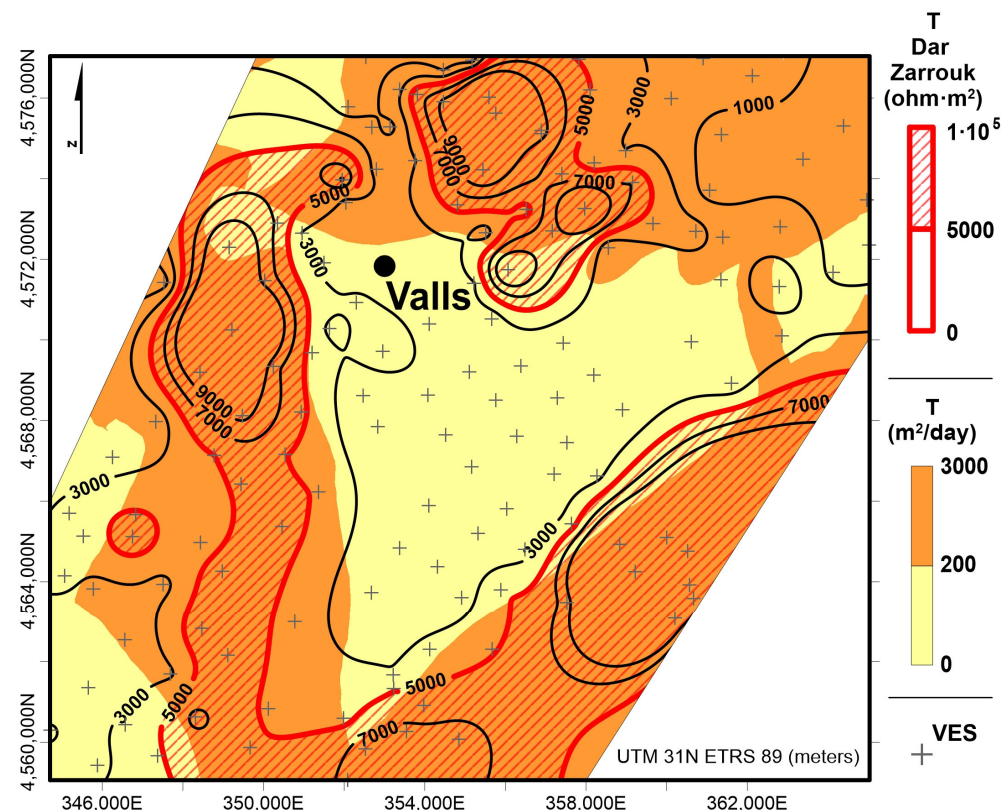


**Figure 8.** Contour map with the transverse resistance values ( $T$  Dar Zarrouk) of the study area superimposed on a simplification of the hydraulic transmissivity ( $T$ ) map produced by the Spanish Geological and Mining Survey [32].

#### 4.4. Aquifer Vulnerability

In order to highlight the best-protected areas from pollution, the  $S$  values were plotted on an isoline map made with the Minimum Curvature interpolation method [56]. The map had the same size and used a regular square grid of the same dimensions (30 m side) as the one used to make the  $T$  map. The interpolation was also limited to the areas with sufficient data, and those with no values (NW and SE of the studied rectangle) were excluded.

The longitudinal conductance values of the study area were grouped into two subsets, one with  $S$  below  $0.5 \Omega^{-1}$  (high to very high vulnerability) and the other with  $S$  above  $0.5 \Omega^{-1}$  (medium to very low vulnerability).

Values higher than 0.5 were identified in the NE and NW zones with an NE–SW orientation and in the W margin with the N–S direction. These values indicate that these areas are more protected from pollution (Figure 9a).

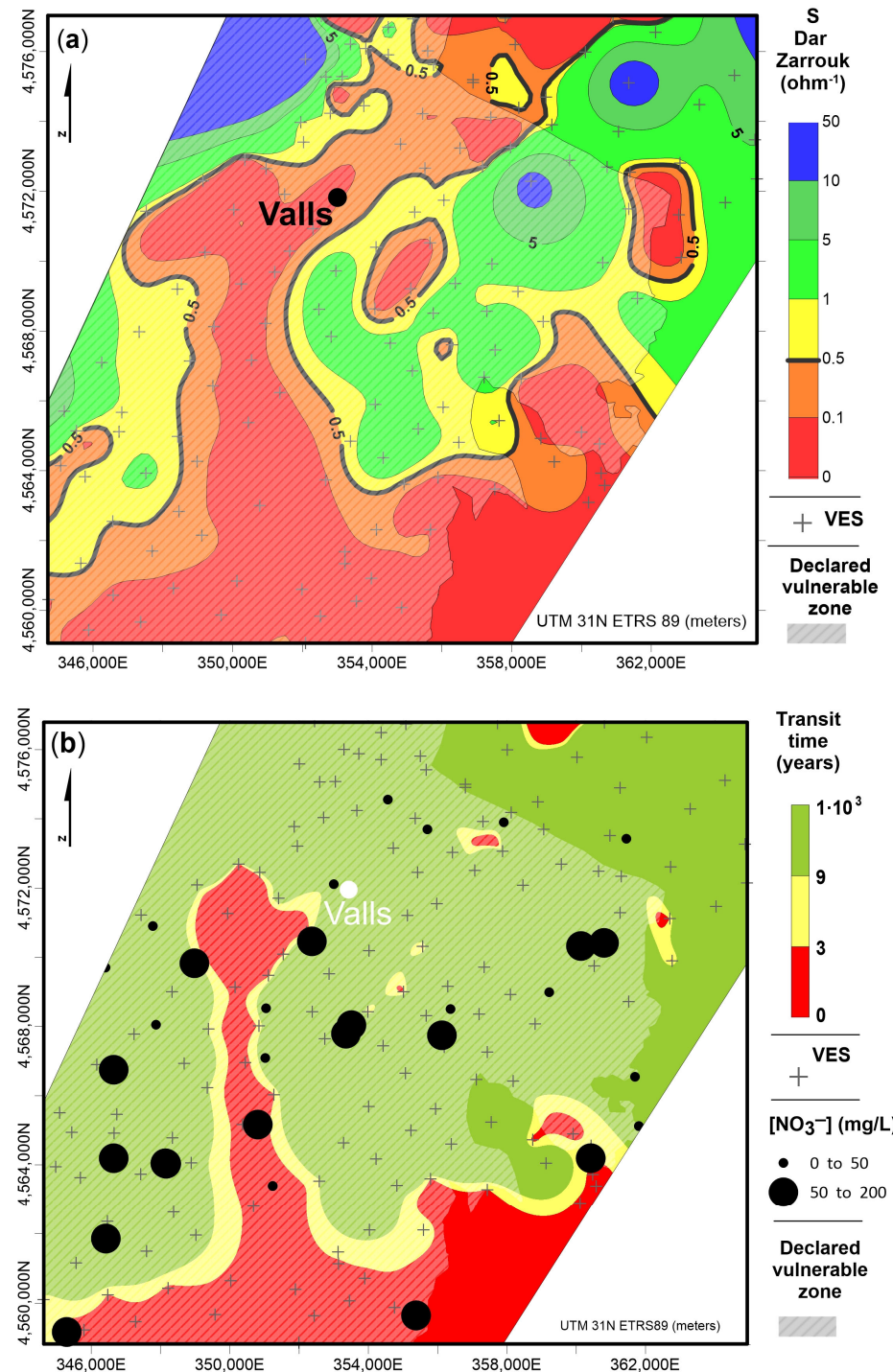


**Figure 9.** (a) Isoline map prepared with the longitudinal conductance values ( $S$  Dar Zarrouk) of the study area; (b) AVI method modified by the authors of [51] and applied to the study area. The black circles represent nitrate concentration data in the wells of the ACA monitoring network [47] and the dashed zone represents those areas declared vulnerable following the Spanish Decree 47/2022 [57].

The lowest  $S$  values are located in the southern part and near the town of Valls, with a NE–SW orientation, and in the central-western area, with an N–S orientation. These values indicate the areas in which the exploited aquifer is more vulnerable to contamination and, in fact, are included in the areas declared as vulnerable to contamination after the implementation of the Spanish Decree [57] and coincide with the observations made by the water basin management organisation [31].

The Dar Zarrouk  $S$  parameter provided a semi-quantitative assessment of the aquifer's vulnerability to contamination, which usually requires a site-specific classification to rate the protective capacity of the unsaturated area [58,59]. The methodology described by the authors of [51] then allowed for a quantitative assessment defining vertical travel times, which was applied to each of the 141 VESs.

To assign the vulnerability categories, the AVI methodology (Table 1) was followed, and the thickness of the unsaturated zone was considered as the difference between the topographic elevation and the piezometric level.

**Table 1.** AVI method aquifer vulnerability categories [50].

Pollutant Transit Time (years)	Vulnerability
0–2	Very high
3–8	Medium-high
>9	Low

The results of this method were interpolated using an ordinary kriging algorithm, adding the values of nitrate concentration in wells (Figure 9b).

Transit times of more than 9 years were identified in the central and northern parts of the studied area, these being, *a priori*, the areas most protected from surface contamination. On the other hand, transit times of less than 3 years, signifying areas very vulnerable to surface contamination were mainly located in the southern part.

The map also shows that 2022 high nitrate values in groundwater (>50 mg/L) [33] were preferentially distributed close to areas with high vulnerability according to their longitudinal electrical conductivity and, thus, their transit time. However, these concentrations depend not only on whether the unsaturated zone is vulnerable to pollution but also on whether there is a potential pollution load from anthropogenic activities [60,61]. Furthermore, the vulnerability map obtained from the use of Dar Zarrouk's parameters allows us to distinguish vulnerable areas even if they fail not show any pollution from dispersed non-assimilated agricultural amendments.

It is necessary to protect these vulnerable areas that contain groundwater resources of good quality to the same or even higher degree than the already polluted areas officially declared vulnerable by the last Spanish Decree 47/2022 [34].

## 5. Conclusions

- The specific treatment carried out on data from geophysical data gravity stations and vertical electric soundings and their reinterpretation, supported by the available well data, has also allowed the hydraulic characteristics of the aquifer system and its vulnerability to contamination through the unsaturated zone to be characterised on a regional scale. Geophysical methods have proved useful in this application, providing valuable information in a non-destructive way, i.e., without the need to drill new boreholes in the ground that could act as preferential pathways for pollutants into the aquifer.
- The results of the interpretation of the VES curves are consistent with the available lithological information on the subsoil and have a better spatial distribution in the study area than the lithological information. Thus, it has been identified that the most favourable areas for the exploitation of groundwater resources are located in the less sinuous sections of the Francolí and Gaià rivers and at the west outskirts of Valls.

- The longitudinal electrical conductance map (Dar Zarrouk S-parameter) effectively shows the protection that exists against groundwater contamination due to the existence of the low vertical permeability of the unsaturated zone, i.e., the uppermost layers between the ground surface and the piezometric level. S values above 0.5 Siemens indicate areas where the aquifer system is more protected, while S values below 0.5 Siemens indicate areas with a higher risk of groundwater contamination, either at a particular point or diffused.
- The correlation between the longitudinal electrical conductance (parameter S of Dar Zarrouk) and the resistance of water to vertical flow through the unsaturated zone was used as a quantitative index in the AVI (Aquifer Vulnerability Index) method to evaluate the vulnerability of groundwater pollution and has made it possible to determine the areas most susceptible to pollution according to the transit time from its infiltration on the surface to reach the aquifer. In the Valls Basin, the most vulnerable areas, with transit times of less than 3 years, are located mainly in the southern part of the study area, while the best-protected areas, with transit times of more than 9 years, are located in the central and northern sectors.

**Supplementary Materials:** The following supporting information can be downloaded at: <https://www.mdpi.com/article/10.3390/w15234130/s1>. Supplementary Material S1: VES location, inferred water table and VES model RMS; Supplementary Material S2: VES models.

**Author Contributions:** Conceptualisation, A.C.; methodology, A.S., M.H. and A.C.; formal analysis, A.S. and A.C.; data curation, A.S., M.H. and A.C.; writing—original draft preparation, A.S.; writing—review and editing A.S., M.H., R.L., L.R., A.U., J.C.T. and A.C. All authors have read and agreed to the published version of the manuscript.

**Funding:** This research received no external funding.

**Data Availability Statement:** The data presented in this study are available on request from the corresponding author.

**Acknowledgments:** We thank Mireia Iglesias, Blanca Torras and Josep Fraile from Catalan Water Agency (ACA), Margarita Valverde from FCIHS and Josep Torrens for their assistance and providing lithological and hydrogeological data.

**Conflicts of Interest:** The authors declare no conflict of interest.

## References

1. European Parliament and Council Comission Directive 2014/101/EU of 30 October 2014 Amending Directive 2000/60/EC Establishing a Framework for Community Action in the Field of Water Policy. Available online: <https://eur-lex.europa.eu/legal-content/EN/TXT/HTML/?uri=CELEX:32014L0101> (accessed on 13 October 2023).
2. European Parliament and Council Directive 2006/118/EC of 12 December 2006 on the Protection of Groundwater Against Pollution and Deterioration. Available online: <https://eur-lex.europa.eu/legal-content/EN/TXT/HTML/?uri=CELEX:02006L0118-20140711> (accessed on 10 October 2023).
3. Duijvenbooden, W.; Waegenringh, H.G.; Foster, S.S.D. Vulnerability of soil and groundwater to pollutants. In Proceedings of the Fundamental Concepts in Aquifer Vulnerability, Pollution Risk and Protection Strategy, Noordwijk Aan Zee, The Netherlands, 30 March 1987; TNO Committee on Hydrological Research: Noordwijk aan Zee, The Netherlands, 1987; p. 1143.
4. Voigt, H.; Heinkele, T.; Jahnke, C.; Wolter, R. Characterization of groundwater vulnerability to fulfill requirements of the water framework directive of the European. *Geofisica Int.* **2004**, *43*, 567–574. [[CrossRef](#)]
5. Galperin, Y.; Odencrantz, J.E. Biodegradation dynamics disparity between n-alkanes and polycyclic aromatic hydrocarbons in the vadose zone: A critical review. *Remediat. J.* **2022**, *32*, 119–128. [[CrossRef](#)]
6. Feng, S.-J.; Zhu, Z.-W.; Chen, H.-X.; Chen, Z.-L.; Ding, X.-H. Two-dimensional analytical solution for subsurface volatile organic compounds vapor diffusion from a point source in layered unsaturated zone. *J. Contam. Hydrol.* **2021**, *243*, 103916. [[CrossRef](#)]
7. Aind, D.A.; Malakar, P.; Sarkar, S.; Mukherjee, A. Controls on Groundwater Fluoride Contamination in Eastern Parts of India: Insights from Unsaturated Zone Fluoride Profiles and AI-Based Modeling. *Water* **2022**, *14*, 3220. [[CrossRef](#)]
8. Gogu, R.C.; Dassargues, A. Current trends and future challenges in groundwater vulnerability assessment using overlay and index methods. *Environ. Geol.* **2000**, *39*, 549–559. [[CrossRef](#)]
9. Vrba, J.; Zaporozec, A. *Guidebook on Mapping Groundwater Vulnerability. International Contributions to Hydrogeology*; International Association of Hydrogeologists: Hannover, Germany, 1994; ISBN 978-3922705970.

10. Hashimoto, T.; Stedinger, J.R.; Loucks, D.P. Reliability, resiliency, and vulnerability criteria for water resource system performance evaluation. *Water Resour. Res.* **1982**, *18*, 14–20. [[CrossRef](#)]
11. Casas, A.; Himi, M.; Díaz, Y.; Pinto, V.; Font, X.; Tapias, J.C. Assessing aquifer vulnerability to pollutants by electrical resistivity tomography (ERT) at a nitrate vulnerable zone in NE Spain. *Environ. Geol.* **2008**, *54*, 515–520. [[CrossRef](#)]
12. Aller, L.; Bennett, T.; Lehr, J.H.; Petty, R.J.; Hackett, G. NWWA/EPA-600/2-87-035. DRASTIC: A Standardized Method for Evaluating Ground Water Pollution Potential Using Hydrogeologic Settings. EPA: Washington, DC, USA, 1987; p. 455.
13. Civita, M.; De Maio, M. *SINTACS: Un Sistema Parametrico per la Valutazione E la Cartografia delle Vulnerabilità Degli Acquiferi All’Inquinamento. Metodologia e Automatizzazione*; Pitagora Editrice: Bologna, Italy, 1997; ISBN 9788837108991.
14. Chachadi, A.G.; Lobo-Ferreira, J.-P. Sea water intrusion vulnerability mapping of aquifers using the GALDIT method. In Proceedings of the UNESCO-IHP Workshop on Modelling in Hydrogeology, Chennai, India, 3 December 2001; Volume 4, pp. 7–9.
15. Khosravi, K.; Bordbar, M.; Paryani, S.; Saco, P.M.; Kazakis, N. New hybrid-based approach for improving the accuracy of coastal aquifer vulnerability assessment maps. *Sci. Total Environ.* **2021**, *767*, 145416. [[CrossRef](#)]
16. Andersen, L.J.; Gosk, E. Applicability of vulnerability maps. *Environ. Geol. Water Sci.* **1989**, *13*, 39–43. [[CrossRef](#)]
17. Kumar, S.; Thirumalaivasan, D.; Radhakrishnan, N.; Mathew, S. Groundwater vulnerability assessment using SINTACS model. *Geomat. Nat. Hazards Risk* **2013**, *4*, 339–354. [[CrossRef](#)]
18. Jury, W.A.; Horton, R. *Soil Physics*, 6th ed.; John Wiley & Sons, Inc.: New York, NY, USA, 2004; ISBN 978-0-471-05965-3.
19. Henriet, J.P. Direct applications of the Dar Zarrouk parameters in ground water surveys. *Geophys. Prospect.* **1976**, *24*, 344–353. [[CrossRef](#)]
20. Kirsch, R. Groundwater protection: Vulnerability of aquifers. In *Groundwater Geophysics. A Tool for Hydrogeology*; Kirsch, R., Ed.; Springer: Berlin, Germany, 2009; pp. 511–525. ISBN 978-3-540-88404-0.
21. Kirsch, R.; Sengpiel, K.-P.; Voss, W. The use of electrical conductivity mapping in the definition of an aquifer vulnerability index. *Near Surf. Geophys.* **2003**, *1*, 13–19. [[CrossRef](#)]
22. Mohammadi, K.; Niknam, R.; Majd, V.J. Aquifer vulnerability assessment using GIS and fuzzy system: A case study in Tehran-Karaj aquifer, Iran. *Environ. Geol.* **2009**, *58*, 437–446. [[CrossRef](#)]
23. George, N.J. Integrating hydrogeological and second-order geo-electric indices in groundwater vulnerability mapping: A case study of alluvial environments. *Appl. Water Sci.* **2021**, *11*, 1–12. [[CrossRef](#)]
24. Bernardo, B.; Candeias, C.; Rocha, F. Integration of Electrical Resistivity and Modified DRASTIC Model to Assess Groundwater Vulnerability in the Surrounding Area of Hulene-B Waste Dump, Maputo, Mozambique. *Water* **2022**, *14*, 1746. [[CrossRef](#)]
25. Niwas, S.; Singhal, D.C. Estimation of aquifer transmissivity from Dar-Zarrouk parameters in porous media. *J. Hydrol.* **1981**, *50*, 393–399. [[CrossRef](#)]
26. Soupios, P.; Kouli, M.; Vallianatos, F.; Vafidis, A.; Stavroulakis, G. Estimation of aquifer hydraulic parameters from surficial geophysical methods: A case study of Keritis Basin in Chania (Crete–Greece). *J. Hydrol.* **2007**, *338*, 122–131. [[CrossRef](#)]
27. Batte, A.G.; Barifaijo, E.; Kiberu, J.M.; Kawule, W.; Muwanga, A.; Owor, M.; Kisekulo, J. Correlation of Geoelectric Data with Aquifer Parameters to Delineate the Groundwater Potential of Hard rock Terrain in Central Uganda. *Pure Appl. Geophys.* **2010**, *167*, 1549–1559. [[CrossRef](#)]
28. Sendrós, A.; Himi, M.; Lovera, R.; Rivero, L.; Garcia-Artigas, R.; Urruela, A.; Casas, A. Geophysical Characterization of Hydraulic Properties around a Managed Aquifer Recharge System over the Llobregat River Alluvial Aquifer (Barcelona Metropolitan Area). *Water* **2020**, *12*, 3455. [[CrossRef](#)]
29. Cobourn, K.M.; Elbakidze, L.; Ghosh, S. *Chapter 3.1.2-Conjunctive Water Management in Hydraulically Connected Regions in the Western United States*; Ziolkowska, J.R., Peterson, J.M.B.T.-C., Eds.; Elsevier: Amsterdam, The Netherlands, 2017; pp. 278–297. ISBN 978-0-12-803237-4.
30. ICGC. *Alt Camp. Mapa Geològic Comarcal de Catalunya 1:50 000*; Institut Cartogràfic i Geològic de Catalunya: Barcelona, Spain, 2005.
31. ACA. *Massa D’Aigua 25. Alt Camp. Fitxa de Caracterització, anàlisi de Pressions, Impacts I anàlisi del Risc D’Incompliment*; Agència Catalana de l’Aigua. Generalitat de Catalunya: Barcelona, Spain, 2004.
32. López-Geta, J.A.; Ramos, G.; Fernández, M.L.; Peinado, T.; Rodríguez, L.; Torrens, J.; Solesillo, J.; Alfonso, P.L.; Fernández, G.; Batlle, A. *Estudio de Los Recursos Hídricos Subterráneos del Sistema Hidrogeológico 74. Camp de Tarragona*, 1st ed.; Instituto Geológico y Minero de España: Madrid, Spain, 1986; ISBN 84-7474-347-8.
33. ACA Catalonia Water Quantity Control Data. Agència Catalana de l’Aigua. *Departament de Territori i Sostenibilitat. Generalitat de Catalunya*. Available online: <http://aca-web.gencat.cat/sdim21/> (accessed on 5 October 2023).
34. ACA. *Zones Vulnerables a la Contaminació per Nitrats Procedents de Fonts Agràries. Fitxes de Les Zones Vulnerables*; Agència Catalana de l’Aigua. Generalitat de Catalunya: Barcelona, Spain, 2022.
35. Telford, W.M.; Geldart, L.P.; Sheriff, R.E. *Applied Geophysics*, 2nd ed.; Cambridge University Press: Cambridge, UK, 1990; ISBN 9780521339384.
36. LCPC. *Détection de Cavités Souterraines Par Méthodes Géophysiques*; Laboratoire Central des Ponts et Chaussées. Institut Français des Sciences et Techniques des Réseaux, de l’Aménagement et des Transport: Marne la Vallée, France, 2004; ISBN 2-7208-0374-X.
37. LaFehr, T.R. Standardization in gravity reduction. *Geophysics* **1991**, *56*, 1170–1178. [[CrossRef](#)]
38. Griffiths, D.H.; Barker, R.D. Two-dimensional resistivity imaging and modelling in areas of complex geology. *J. Appl. Geophys.* **1993**, *29*, 211–226. [[CrossRef](#)]

39. Cimino, A.; Cosentino, C.; Oieni, A.; Tranchina, L. A geophysical and geochemical approach for seawater intrusion assessment in the Acquedolci coastal aquifer (Northern Sicily). *Environ. Geol.* **2008**, *55*, 1473–1482. [[CrossRef](#)]
40. McInnis, D.; Silliman, S.; Boukari, M.; Yalo, N.; Orou-Pete, S.; Fertenbaugh, C.; Sarre, K.; Fayomi, H. Combined application of electrical resistivity and shallow groundwater sampling to assess salinity in a shallow coastal aquifer in Benin, West Africa. *J. Hydrol.* **2013**, *505*, 335–345. [[CrossRef](#)]
41. Canzoneri, A.; Capizzi, P.; Martorana, R.; Albano, L.; Bonfardeci, A.; Costa, N.; Favara, R. Geophysical Constraints to Reconstructing the Geometry of a Shallow Groundwater Body in Caronia (Sicily). *Water* **2023**, *15*, 3206. [[CrossRef](#)]
42. Orellana, E. *Prospección Geoeléctrica en Corriente Continua*, 2nd ed.; Thomson Paraninfo: Madrid, Spain, 1982; ISBN 9788428311533.
43. Interpex. *RESIX PLUS v2.53. User Manual Resistivity Data Interpretation Software*; Interpex Limited: Golden, CO, USA, 1993.
44. Inman, J.R. Resistivity inversion with ridge regression. *Geophysics* **1975**, *40*, 798–817. [[CrossRef](#)]
45. Maillet, R. The fundamental equations of electrical prospecting. *Geophysics* **1947**, *12*, 529–556. [[CrossRef](#)]
46. Edwards, L.S. A modified pseudosection for resistivity and IP. *Geophysics* **1977**, *42*, 1020–1036. [[CrossRef](#)]
47. ACA Catalonia Water Quality Control Data. Agència Catalana de l'Aigua. Departament de Territori i Sostenibilitat. Generalitat de Catalunya. Available online: <http://aca-web.gencat.cat/sdim21/> (accessed on 2 November 2021).
48. Davis, J.C. *Statistics and Data Analysis in Geology*, 3rd ed.; Wiley: New York, NY, USA, 2002; ISBN 978-0-471-17275-8.
49. Sendrós, A.; Díaz, Y.; Himi, M.; Tapias, J.C.; Rivero, L.; Font, X.; Casas, A. An evaluation of aquifer vulnerability in two nitrate sensitive areas of Catalonia (NE Spain) based on electrical resistivity methods. *Environ. Earth Sci.* **2014**, *71*, 77–84. [[CrossRef](#)]
50. Stempvoort, D.; Van Ewert, L.; Wassenaar, L. Aquifer Vulnerability Index: A GIS-compatible method for groundwater vulnerability mapping. *Can. Water Resour. J.* **1993**, *18*, 25–37. [[CrossRef](#)]
51. Kalinski, R.J.; Kelly, W.E.; Bogardi, I.; Pesti, G. Electrical resistivity measurements to estimate travel times through unsaturated ground water protective layers. *J. Appl. Geophys.* **1993**, *30*, 161–173. [[CrossRef](#)]
52. Agarwal, B.N.P. Direct gravity interpretation of sedimentary basin using digital computer—Part I. *Pure Appl. Geophys.* **1971**, *86*, 5–12. [[CrossRef](#)]
53. Casas, A.; Torné, M.; Banda, E. *Mapa Gravimètric de Catalunya 1:500.000*; Servei Geològic de Catalunya. Departament de Política Territorial i Obres Públiques: Barcelona, Spain, 1986; ISBN 978-84-393-0740-2.
54. Guimerà, J.J. *Estudi estructural de L'Enllaç Entre la Serralada Ibèrica i la Serralada Costanera Catalana*; Universitat de Barcelona: Barcelona, Spain, 1988.
55. Bovachev, A.A.; Modin, I.N.; Shevnin, V.A. *1D Interpretation of VES profile software (IPI2Win v3.0.1)*; Moscow State University, Department of Geophysics: Moscow, Russia, 2011.
56. Smith, W.H.F.; Wessel, P. Gridding with continuous curvature splines in tension. *Geophysics* **1990**, *55*, 293–305. [[CrossRef](#)]
57. MPRCMD. *Real Decreto 47/2022, de 18 de Enero, Sobre Protección de Las Aguas Contra la Contaminación Difusa Producida Por Los Nitratos Procedentes de Fuentes Agrarias*; Ministerio de la Presidencia, Relaciones con las Cortes y Memoria Democrática. Gobierno de España: Madrid, Spain, 2022.
58. Alabi, O.O.; Ojo, A.O.; Akinpelu, D.F. Geophysical Investigation for Groundwater Potential and Aquifer Protective Capacity around Osun State University (UNIOSUN) College of Health Sciences. *Am. J. Water Resour.* **2016**, *4*, 137–143. [[CrossRef](#)]
59. Sendrós, A.; Himi, M.; Estévez, E.; Lovera, R.; Palacios-Díaz, M.P.; Tapias, J.C.; Cabrera, M.C.; Pérez-Torrado, F.J.; Casas, A. Hydrogeophysical Assessment of the Critical Zone below a Golf Course Irrigated with Reclaimed Water close to Volcanic Caldera. *Water* **2021**, *13*, 2400. [[CrossRef](#)]
60. Zaporozec, A.; Miller, J.C. *Ground-Water Pollution*; United Nations Educational, Scientific and Cultural Organization: Paris, France, 2000.
61. Debernardi, L.; De Luca, D.A.; Lasagna, M. Correlation between nitrate concentration in groundwater and parameters affecting aquifer intrinsic vulnerability. *Environ. Geol.* **2008**, *55*, 539–558. [[CrossRef](#)]

**Disclaimer/Publisher's Note:** The statements, opinions and data contained in all publications are solely those of the individual author(s) and contributor(s) and not of MDPI and/or the editor(s). MDPI and/or the editor(s) disclaim responsibility for any injury to people or property resulting from any ideas, methods, instructions or products referred to in the content.